23rd ABCM International Congress of Mechanical Engineering
December 6-11, 2015, Rio de Janeiro, RJ, Brazil

# RECONFIGURABLE SYSTEMS IN THE MODELING OF WELD BEAD WIDTH IN THE GMAW PROCESS.

**Edna Margarita Moncayo Torres,**
emmoncayo@unb.br
**Jorge Andrés Girón Cruz,**
University of Brasilia, Department of Mechanical Engineering, Brasília, DF, 70910-900, Brazil.
jorgeandres@unb.br

**Sadek C. Absi Alfaro**
sadek@unb.br
University of Brasilia, Department of Mechanical Engineering, Brasília, DF, 70910-900, Brazil.

***Abstract.*** *In the Gas Metal Arc Welding process the balance between the input parameters characterize the metal transfer modes and influences the geometry, microstructure and mechanical properties of the welded joint. For this reason, the correct selection of the values for the input parameters play an important role in determining welding quality. In the present study, the welding process control is realized with a DE2-115 Altera FPGA. The integrated control system based on a desired width predicted values for the wire feed rate, welding speed and voltage. Central composite design (CCD), together with linear regression, was successfully used to modeling the weld bead width, in order to determine the influence of the process variables on it geometric characteristic.*

***Keywords:*** *Gas Metal Arc Welding (GMAW), reconfigurable systems, central composite design , linear regression.*

## 1. INTRODUCTION

The Gas Metal Arc Welding (GMAW) has become widely used in the manufacturing of all kinds of industrial processes, due to its advantages regarding to other existing techniques. The weld bead geometry is extremely important in the mechanical properties determination of the weld process (Ghalib *et al.*, 2012). The variables on the weld bead geometry, such as width, penetration and reinforcement, are influenced by operating parameters such as, current, voltage and welding speed - among the most important. Many authors study the relationship between the welding process parameters with the weld bead geometry for getting response function models (Gomes *et al.*, 2012).

A common approach to achieve the optimum welding parameters is to build mathematical models linking the process response with the input variables; its design is carried out through either analytical or empirical approaches. The analytical approaches usually includes from simple models, based on the force analysis acting on a drop of weld metal (Lima *et al.*, 2005) to highly complex models, as well as high-level computer simulations (Xu *et al.*, 2009). Despite the many investigations carried out to analyze the arc welding processes, currently, there is a lack of correct and general models to relate the input parameters and the weld bead geometry due to its novelty and its high production method.

On the other hand, there is currently a high demand for embedded systems that not only allows achieve high-performance computing tasks, but also meets robustness requirements, fault tolerance, low cost and power consumption. Several applications of FPGAs (Field-programmable Gate Arrays) in robotics (as part of embedded system modules) appeared in recent years. The direct mapped in hardware algorithm in FPGAs achieves speeds between 10 and 100 times compared with the same algorithm in software. The Field-programmable Gate Arrays (FPGA) offers many benefits as flexibility, high performance, variable bits width and high degree of instructions parallelism (Gokhale and Graham, 2005).

In this way, the present study develops an embedded system that handles the communication between the FPGA DE2 115 (Altera) and the welding process. Response surface methodology (RSM) is used to develop statistical models of weld bead width and, to obtain this statistical model is developed a central composite design (CCD) for the experimental setup. In order to establish the effect of the process parameters on the bead width, are defined as input variables the wire feed rate, the welding speed and the voltage, because its major influence on the weld bead geometry. With the models found from a pre-defined width is possible to predict the optimum values for the input parameters.

## 2. LITERATURE REVIEW

### 2.1. Gas metal arc welding GMAW

Gas metal arc welding (GMAW) is an electric arc welding process that fuses together the parts to be welded by heating them with an arc between a solid metal electrode and the work piece. Filler metal is obtained from melting of the electrode wire, which is fed continuously into the arc by the welding equipment. Shielding is obtained from an externally supplied gas or gas mixture (Modenesi, *et. al*., 2012). The reasons for accepting GMAW for almost all industrial applications are due to its versatility and advantages as; GMAW process is easily adapted for high-speed robotic, hard automation and semiautomatic welding applications; lower heat input when compared to other welding processes; generally, lower cost per length of weld metal deposited when compared to other open arc welding processes.

### 2.2. Weld Bead Geometry

In the field of welding, weld quality mainly depends on the mechanical properties of the weld metal and heat affected zone, which in turn, is influenced by metallurgical characteristics and chemical compositions of the weld. Moreover, these mechanical-metallurgical features depend on the weld bead geometry, which are directly related to welding process parameters (Esme *et al.* 2009), hence, study and control of weld bead shape is essential and relationships between the process parameters and the weld bead geometry characteristics are often established. Some important geometrical characteristics of the weld beads in study are shown in Fig. 1. In order to achieve online control, this work focuses on external characteristics; width, reinforcement and area of weld bead (cross section of surface).

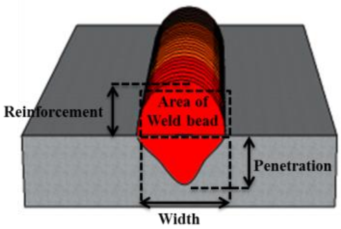


Figure 1: Weld Bead Geometry Characteristics.

### 2.3. field-programmable gate array (FPGA)

FPGAs, as illustrated in Fig. 2, consist of an array of programmable logic blocks of potentially different types, including general logic, memory and multiplier blocks, surrounded by a programmable routing fabric that allows blocks to be programmable interconnected. The array is surrounded by programmable input/output blocks, labeled I/O in the figure, that connect the chip to the outside world. The "programmable" term in FPGA indicates ability to program a function into the chip after silicon fabrication is complete. This customization is possible by the programming technology, which is a method that cause a change in the behavior of the pre-fabricated chip after fabrication, in the "field," where system users create designs (Vallejo and Rodrigo, 2004).

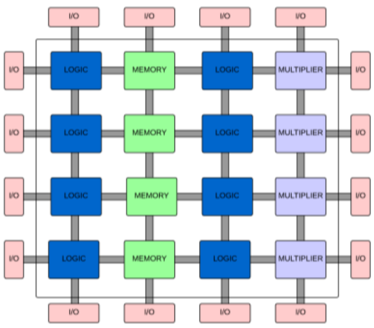


Figure 2: Basic FPGA structure.

### 2.4. Response Surface Methodology

An important subject in the statistical design of experiments is the Response Surface Methodology (RSM), this is a collection of mathematical and statistical techniques useful for the modeling and analysis of systems whose output is influenced by several variables and its goal is to optimize this response (Richetti, 2003). Based on experimental design, a multiple linear regression technique is used to get second-order models, which can be written as in Eq. (1), where $y$

represents the response and $x$ the input variable. The $b$ terms are called regression coefficients and represent the parameters that define the model (Myers, *et al*. 2009).

$$y = b_0 + b_1x_1 + b_2x_2 + b_3x_3 + b_{11}x_1^2 + b_{22}x_2^2 + b_{33}x_3^2 + b_{12}x_1x_2 + b_{13}x_1x_3 + b_{23}x_2x_3 \quad (1)$$

## 3. METHODOLOGY

The methodology used in the study has two steps, as shown in Fig. 3, below.

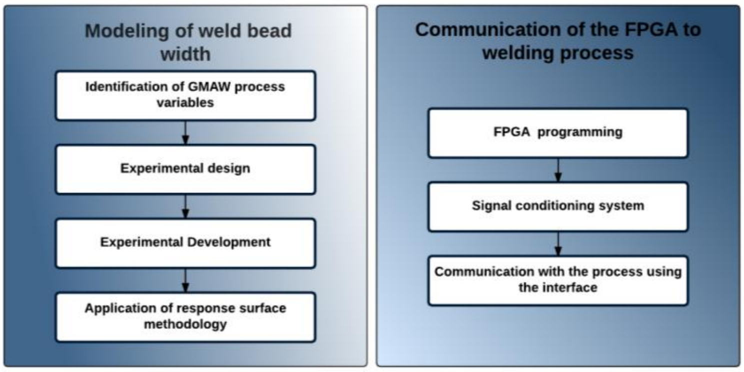


Figure 3: The methodology used in the present study.

### 3.1. Modeling of weld bead width

#### 3.1.1. Identification of GMAW process variables

The mechanical properties of the weld bead depend on its geometric parameters, which in turn, are dependent on the input process parameters. In this work are taken account the variables which direct action and its interaction have a significant influence on the external geometry of the weld bead. Then, voltage, wire feed rate and welding speed were established as input variables.

#### 3.1.2. Experimental design

As there is no defined a methodology to choose the number of trial runs, in this study made use of Central Composite Design (CCD), as show fig. 4, in order to examine the behavior of the response variables in the experimental runs. The CCD counts with a factorial design $2^3$ increased with six axial points and a central point. Experiments were carried out with the variations in the process parameters based on experimental design to evaluate the influence on the weld bead geometry. Table 1 shows the coded factor levels and their corresponding values to each selected process parameters.

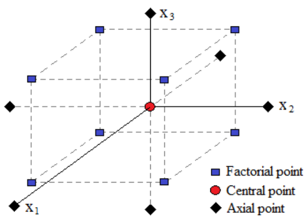


Figure 4: Central composite design for three input variables.

Table 1: Ranges and levels of the welding variables selected for the CCD.

| **Welding parameters** | **Symbol** | **Ranges and Levels** | | | | |
|---|---|---|---|---|---|---|
| | | **-1.682** | **-1** | **0** | **1** | **1.682** |
| Wire feed rate (m/min) | $x_1$ | 4.8 | 5.5 | 6.5 | 7.5 | 8.2 |
| Voltaje (V) | $x_2$ | 16.2 | 19 | 23 | 27 | 29.7 |
| Welding speed (mm/s) | $x_3$ | 6.6 | 8 | 10 | 12 | 13.4 |

With the combination of variables values listed in the Tab. 1 was performed the experimental matrix displayed in Tab. 2, here are indicated the selected experiments and the values for each variable.

Table 2: Values of the variables considered in the preparation of the matrix of experiments.

| No Exp | Levels | | | Ranges | | | No Exp | Levels | | | Ranges | | |
|---|---|---|---|---|---|---|---|---|---|---|---|---|---|
| | $x_1$ | $x_2$ | $x_3$ | $x_1$ | $x_2$ | $x_3$ | | $x_1$ | $x_2$ | $x_3$ | $x_1$ | $x_2$ | $x_3$ |
| **1** | -1 | -1 | -1 | 5.5 | 19 | 8 | **11** | 0 | -1.682 | 0 | 6.5 | 16.3 | 10 |
| **2** | 1 | -1 | -1 | 7.5 | 19 | 8 | **12** | 0 | 1.682 | 0 | 6.5 | 29.7 | 10 |
| **3** | -1 | 1 | -1 | 5.5 | 27 | 8 | **13** | 0 | 0 | -1.682 | 6.5 | 23 | 6.6 |
| **4** | 1 | 1 | -1 | 7.5 | 27 | 8 | **14** | 0 | 0 | 1.682 | 6.5 | 23 | 13.4 |
| **5** | -1 | -1 | 1 | 5.5 | 19 | 12 | **15** | 0 | 0 | 0 | 6.5 | 23 | 10 |
| **6** | 1 | -1 | 1 | 7.5 | 19 | 12 | **16** | 0 | 0 | 0 | 6.5 | 23 | 10 |
| **7** | -1 | 1 | 1 | 5.5 | 27 | 12 | **17** | 0 | 0 | 0 | 6.5 | 23 | 10 |
| **8** | 1 | 1 | 1 | 7.5 | 27 | 12 | **18** | 0 | 0 | 0 | 6.5 | 23 | 10 |
| **9** | -1.682 | 0 | 0 | 4.8 | 23 | 10 | **19** | 0 | 0 | 0 | 6.5 | 23 | 10 |
| **10** | 1.682 | 0 | 0 | 8.2 | 23 | 10 | **20** | 0 | 0 | 0 | 6.5 | 23 | 10 |

### 3.1.3. Experimental Development

The materials used in the experimental setup are: Solid wire AWS A5.18 ER70S-type 6 with a diameter of 1 mm; base material steel AISI 1020; distance from contact tube to the workpiece 16 mm; shielding gas 96% Ar and 4% CO2; shielding gas flow rate 15 liters / min; welding source Fronius Trans Plus Synergic 5000; slide table developed by Franco, (2008).

The present work aims to achieve the modeling of weld bead width, in order to that, are made the same experiments as shown in Tab. 2, obtaining a measure of the bead width for each of the combinations.

For the geometrical parameters measurement is used an optical scanning system consisting of a line shape laser and a webcam. The device is run through the weld bead and by using digital image processing is obtained a 3D reconstruction of the weld (Torres, *et al*, 2013), as shown in Fig 5. From the 3D reconstruction are obtained two measures for each output variable in the weld bead (width, reinforcement, and area), the first being the average of each measurement, regardless the limits of the bead, and the second the error measure with respect to the non-uniformity of the weld bead (standard deviation of measure), as shown in Fig 6.

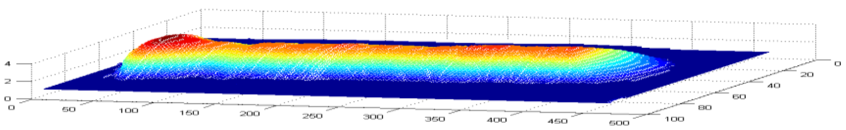

Figure 5: Reconstruction in 3D of the weld bead.

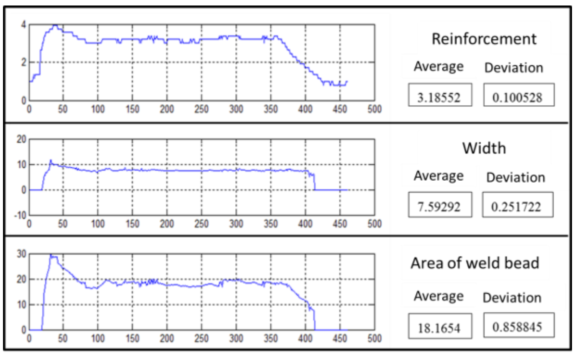


Figure 6: Measurements of geometrical parameters.

### 3.1.4. Application of response surface methodology

The response surface methodology is developed from the Tab. 2. Then, the weld bead width and the standard deviation model are found. From these models the optimal parameters are found for a predefined weld bead width using the sequence shown in Fig. 7.

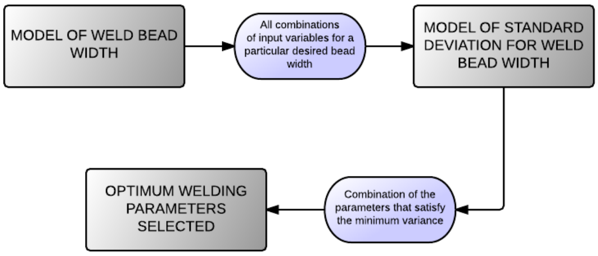


Figure 7: Sequence to obtain the optimal parameters.

### 3.2. Communication of the FPGA to welding process

#### 3.2.1. FPGA programming

In the present study is used a TERASIC KIT VEEK MT including a FPGA DE2 115 of Altera, a remote control and a LCD screen. The General Purpose Input/Output (GPIO) is programmed for input and output signals, this port is a generic pin on an integrated circuit whose behavior, including whether it is an input or output pin, can be controlled by the user at run time, this port has an output of 3.3 V.

An 8-bit word is defined for the process variables: voltage, wire feed rate and welding speed. Moreover the digital outputs for controlling the welding source and the slide table are defined. The remote control permit to choose the desired bead width and the other process parameters. The LCD screen shows the sequence of actions being executed, such as, the desired bead width chosen, the direction of the slide table selected, welding time, the parameters to initialize the source welding and the status of the process.

#### 3.2.2. Signal conditioning system

To perform the communication between the FPGA and the welding process is implemented a signal conditioning system, with operational amplifiers, digital to analog converters and solid-state relays. The system consists of 20 digital inputs from 0 to 3.3 volts (signals from FPGA), 2 analog outputs of 0-10 volts, 1 analog output of 0-5 volts, 2 digital outputs of 0-5 volts and 2 digital outputs of 0-24 volts.

#### 3.2.3. Communication with the process using the interface

The communication is performed by the Fronius ROB 5000 interface and a microcontroller (PIC16C63A) to control the variables of welding source and slide table respectively in real-time. The ROB 5000 interface has analog inputs and outputs in a range of 0 to 10 volts and digital inputs and outputs in a range of 0 to 24 volts. The digital signals are used to start the source in order to start the welding process; the analog inputs are used to control the wire feed rate and voltage. As settled before it has a range of 0 to 10 volts equivalents 0-22 m/min and 0 to 40 volts, respectively. The microcontroller is responsible for slide table rate control including direction, welding speed and start time.

## 4. RESULTS

### 4.1. Experimental development

Table 3 shows the results of the measurements of bead width obtained from the experiments indicated in Tab. 2.

Table 3: Results of the experiments.

| No Exp | 1 | 2 | 3 | 4 | 5 | 6 | 7 | 8 | 9 | 10 | 11 | 12 | 13 | 14 | 15 | 16 | 17 | 18 | 19 | 20 |
|---|---|---|---|---|---|---|---|---|---|---|---|---|---|---|---|---|---|---|---|---|
| Average | 5.9 | 6.7 | 7.6 | 8.8 | 5.1 | 5.4 | 5.7 | 6.7 | 5.7 | 7.2 | 4.9 | 7.7 | 8.6 | 5.4 | 6.5 | 6.7 | 6.5 | 6.7 | 6.7 | 6.5 |
| Standard deviation | 0.2 | 0.2 | 0.6 | 0.5 | 0.2 | 0.4 | 0.7 | 0.4 | 0.6 | 0.5 | 0.9 | 0.4 | 0.5 | 0.5 | 0.7 | 0.9 | 0.7 | 0.8 | 0.7 | 0.8 |

#### 4.1.1. The response surface methodology

Table 3 shows the values for the weld bead width from these results is obtained the mathematical models of the input variables and responses using the least squares method. Since models are presented in terms of the coded values (-1.682, -1, 0, 1, 1.682), conversion to real values of models are performed using the Eq. (2). Equation (1) represents how to use Eq. (2) in the models, where $x_1$, $x_2$ and $x_3$ are the real values of input variables.

$$\zeta_1 = x_1 - 6.5 \qquad \zeta_2 = \frac{x_2 - 23}{4} \qquad \zeta_3 = \frac{x_3 - 10}{2} \tag{2}$$

Equation (3) shows the models of the bead width.

$$y_L = 6.6723 + 0.4335\zeta_1 + 0.7605\zeta_2 - 0.8518\zeta_3 - 0.0989\zeta_1{}^2 - 0.1421\zeta_2{}^2 + 0.1204\zeta_3{}^2 + 0.1206\zeta_1\zeta_2 - 0.0871\,\zeta_1\zeta_3 - 0.2035\,\zeta_2\zeta_3 \tag{3}$$

Equation (4) represents the model of the bead width error with respect to non-uniformity of the weld bead.

$$y_{EL}{}^* = 0.7657 - 0.0269\,\zeta_1 + 0.0259\zeta_2 + 0.0235\zeta_3 - 0.1039\zeta_1{}^2 - 0.0549\zeta_2{}^2 - 0.1217\zeta_3{}^2 - 0.0580\,\zeta_1\zeta_2 - 0.0166\,\zeta_1\zeta_3 - 0.0261\,\zeta_2\zeta_3 \tag{4}$$

Figure 8 shows the response surface of the weld bead width related to the wire rate and the voltage (constant welding speed, 10 mm/s), here is observed that the bead width increases proportionally with the voltage. The influence of the wire feed rate is that using higher speed is obtained an increase in the bead width.

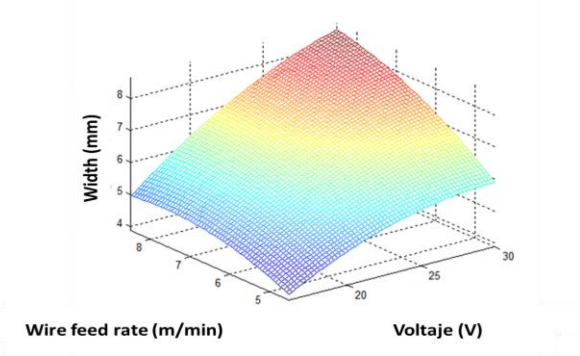


Figure 8: Response surface of the width.

**4.2. Optimal parameters for bead width.**

For the selection of optimal parameters for a specified bead width is used the NIOS II program, this program allows configurable processor programming of the FPGA and presents a programming language C. A program with the model of the bead width was developed with the variables ranged between -1 and 1, these variables were evaluated in all its possible combinations in order to obtain the values for a specific response.

As an example the Fig. 9 shows the possible combinations of the three input variables, to obtain a width of 6 mm.

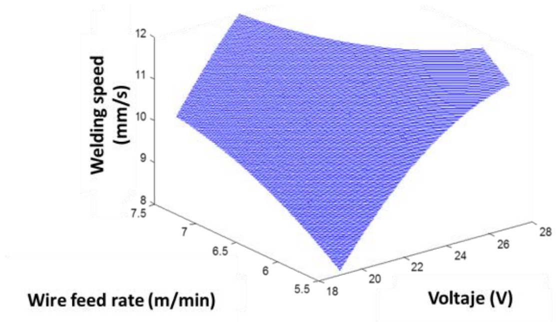


Figure 9: Set of combinations of the input variables for a width of 6 mm.

Once obtained these combinations these are evaluated in the error model with respect to non-uniformity. Since it seeks to find the optimal parameters to generate a weld bead with good appearance and quality, it is chosen the combination that has the smallest error. Table 4 shows some optimal parameters for different measures of the bead width.

Table 4: Optimal parameters for particulars width.

| Width (mm) | Optimal parameters | | |
|---|---|---|---|
| | Voltage (V) | Wire feed rate (m/min) | Weld speed (mm/s) |
| 5 | 19.47 | 5.5 | 12 |
| 5.5 | 23.04 | 5.5 | 12 |
| 6 | 21.94 | 7.5 | 12 |
| 6.5 | 25.06 | 7.5 | 12 |
| 7 | 26.95 | 7.5 | 11.4 |
| 7.5 | 25.47 | 5.5 | 8 |

Figure 10a and Fig. 10b show the weld bead obtained for widths of 5 and 6 mm respectively.


(a)


(b)

Figure 10: Weld bead obtained for widths of (a) 5mm e (b) 6mm.

Figure 11a and Fig. 11b show the 3D reconstruction of the weld bead. Figure 12a presents the measurements of geometric characteristics from a weld bead of 5mm. The result was an average width of 5,03 mm with a standard deviation of 0,47 mm, reinforcement height of 2,03 mm with a standard deviation of 0,095 mm and weld bead area of 8,03 $mm^2$ with a standard deviation of 0,674 $mm^2$ . Figure 12b presents the measurements of geometric characteristics from a weld bead of 6mm. The result was an average width of 6,01 mm with a standard deviation of 0,37 mm, reinforcement height of 2,7 mm with a standard deviation of 0,1 mm and weld bead area of 12,77 $mm^2$ with a standard deviation of 0,91 $mm^2$.

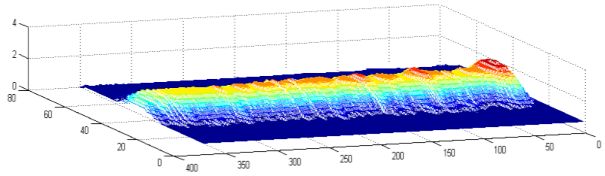
(a)

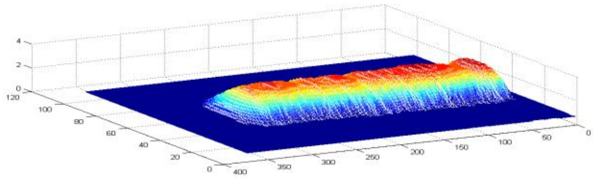
(b)

Figure 11: 3D reconstruction of weld bead with (a) 5mm and (b) 6mm of width

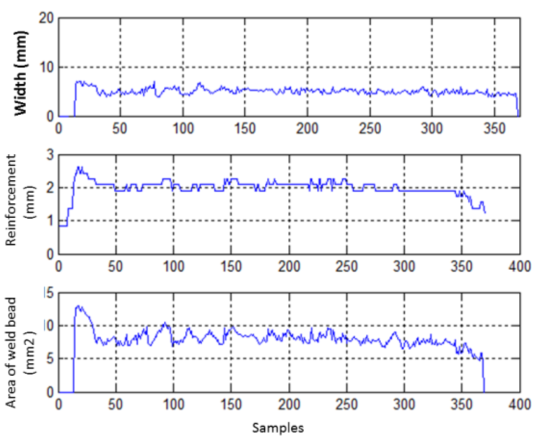

(a)

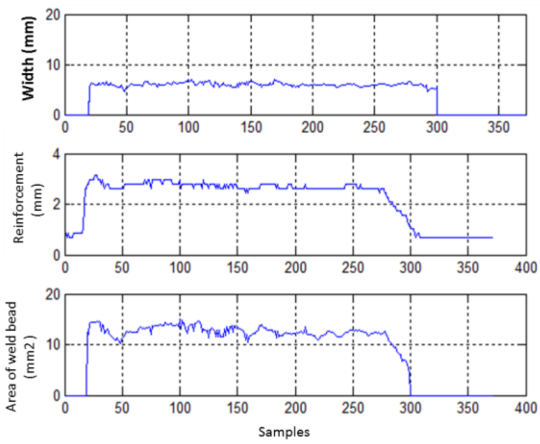

(b)

Figure 12: Geometrical parameters measurement for weld bead of (a) 5 mm and (b) 6mm of width

The system developed for welding parameter prediction from the desired weld bead width, has showed satisfactory results. The accuracy level achieved with use of the system is outlined in Tab. 5 and appears to be acceptable for most common industrial applications, taking into consideration measurement accuracy and the random nature of the material, where W is the desired width in millimeters and WR is the actual width in millimeters.

Table 5: Level of accuracy obtained.

| $W$ | $WR$ | $\|W - WR\|$ | $Error$ % |
|---|---|---|---|
| 5 | 5,03 | 0,03 | 0,6 |
| 6 | 6,01 | 0.01 | 0,16 |
| 7 | 6,93 | 0.07 | 1,01 |

## 5. CONCLUSION

The modeling process developed in the present work can be used as a methodology for obtaining the optimal welding parameters to find the desired bead width. Arc voltage, wire feed rate and welding speed values that optimize the response were found, obtaining welds of good appearance and quality. The model found and developed in the present study predicts in a proper way the welding process parameters for a certain desired bead width.

The mathematical models developed to predict the input variables in weld bead width function are suitable, due to the small deviation obtained for each case. When analyzing the measurements of geometric parameters, it was observed that the cords obtained not only present uniformity in its width, but considering the standard deviations of the three geometric parameters, the obtained beads have uniformity in the three external geometric parameters.

Communicating the welding process is managed with the FPGA, using the packaging system signals and the communication interface. Achieving sending the parameters for the welding source and the slide table in real time.

## 6. REFERENCES

Esme, U., Bayramoglu, M., Kazancoglu, Y., Ozgun, S., 2011. "Optimization of weld bead geometry in welding process using grey relation analysis and taguchi method". *Proceedings of Materials and technology*. Vol. 43, p. 143-149.

Franco, F.D., 2008. "Monitorização e Localização de Defeitos na Soldagem TIG através do Sensoriamento Infravermelho". Dissertação de Mestrado em Sistemas Mecatrônicos, Publicação ENM.DM-026A/08, Departamento de Engenharia Mecânica, Universidade de Brasília, Brasília, DF, 125p.

Ghalib, T., Mohamad, Y., Sunhaji, K., Yupiter, H.; Bukhari, A., 2012. "Predicting the GMAW 3F T-Fillet Geometry and Its Welding Parameter". *International Symposium on Robotics and Intelligent Sensors.* Procedia Engineering 41, p. 1794 – 1799.

Gokhale, M., Graham, P. S., 2005. "Reconfigurable computing - accelerating computation with field programmable gate arrays". *Real-Time Springer Editorial*.

Gomes, J., Costa, S., Paiva, A. e Balestrassi, P., 2012. "Mathematical modeling of weld bead geometry, quality and productivity for stainless steel claddings deposited by FCAW". *Journal of Materials Engineering and Performance*, volume 21, Issue 9, p. 1862-1872.

Lima I.E., Castro, C., Bracarense, A. e Campos, M., 2005. "Determinação da Relação Entre Parâmetros de Soldagem, Largura da Poça e Aspectos do Cordão de Solda Utilizando Câmera de Alta Velocidade". *Soldagem Inspeção*. Vol. 10, No. 4, Out/Dez.

Modenesi, P., Marques, P. e Santos, D., 2012. "Introdução à Metalurgia da Soldagem". Universidade Federal de Minas Gerais, Departamento de Engenharia Metalúrgica e de Materiais, Belo Horizonte.

Myers, R.H., Montgomery, D.C., Anderson-Cook, C., 2009. "Response Surface Methodology, Process and Product Optimization Using Designed Experiments, 3Ed.", *John Wiley & Sons, Inc*. Hoboken, New Jersey, USA, 680 p.

Richetti, A., 2003, "Análise e Modelagem Empírica do Processo de Soldagem a Plasma com "Keyhole" em Aço Inoxidável". Tese de Doutorado, Universidade de Uberlândia, M-G. Brasil.

Torres, E.M.M., Cruz, J.A.G., Lopera, J.E.P., Alfaro, S., 2013. "Parameter optimization in GMAW process with solid and metal-cored wires". *22nd International Congress of Mechanical Engineering (COBEM 2013)*. Ribeirão Preto, SP, Brazil.

Vallejo, M.L., Rodrigo, J.L., 2004. "FPGA: Nociones básicas y Implementación". Departamento de Ingeniería Electrónica. Universidad Computense de Madrid.

Xu, G., Hu, J., Tsai, H.L., 2009. "Three-dimensional modeling of arc plasma and metal transfer in gas metal arc welding." In *Proceedings of the International Journal of Heat and Mass Transfer*, 52, p. 1709-1724.

## 7. RESPONSIBILITY NOTICE

The authors are the only responsible for the printed material included in this paper.